SCC IN HOT WATER ENVIRONMENT - COMPARISON OF SCC MECHANISMS OF TWO BAINITIC STEELS

Anna Brožová, Martin Ruščák, Dana Lauerová*

The CrNiMoV and NiMnMo steels were tested to establish a sensitivity to environmentally assisted cracking in PWR water and in the water oxygen doped. From SSRT it was found that SCC cracks initiate only in high oxygen water in both steels under yield point. The rising displacement test of pre-cracked CT specimens was chosen for crack growth kinetics measurements. SCC was seen in high oxygen for both steel types, but SCC crack growth mechanisms of the steels appear to be dependent on specimen type. The SCC mechanisms of the two steels having been related in case of tensile specimen tests were completely different in CT specimens tests. The paper aims to explain this fact using optical microscopy, SEM and electrochemistry.

INTRODUCTION

It has been recognized for many years that stress corrosion cracking of low-alloy steels can occur under constant load or monotonically increasing strain in hot water environment. For monotonically increasing strain SCC testing slow strain rate tests (SSRT) are commonly used and now a new method - rising displacement test (RDT) based on fracture mechanics J-R curve was proposed to overcome experimental difficulties with long time static testing, e.g. Dietzel (1).

Many models for SCC propagation in the low alloy steel/hot water systems have been developed. The most famous of them the Ford's slip dissolution model (2), has been worked to reliable life prediction methodology. The model mainly takes environment effects into account, implicitly material properties are considered. On the other hand in the enhanced plasticity model, Magnin (4), a local cleavage process plays key role. But the models mentioned describe the SCC in a very similar way and it is difficult to distinguish between them from fractography.

* Nuclear Research Institute Řež, plc., 250 68 Řež, The Czech Republic

EXPERIMENT

The steels CrNiMoV and NiMnMo used as the reactor pressure vessel base material and primary piping material of the nuclear power plant were used for experiments. Table 1 shows the chemical compositions. Microstructure of the CrNiMoV steel was a mixture of tempered bainite with martensite and the NiMnMo steel was a mixture of tempered bainite with proeutektoid ferrite. The austenitic grain sizes were 50 μm in case of the CrNiMoV steel and 35 μm for the NiMnMo steel.

TABLE 1- Chemical composition of the steels.

material	C	Mn	Si	P	S	Ni	Cr	Mo	V	Cu
NiMnMo	0.10	0.80	0.26	0.010	.008	1.92	0.17	0.50	0.04	0.07
CrNiMoV	0.16	0.48	0.28	0.009	.010	1.29	2.20	0.59	0.09	0.06

The experiments were carried out in two test environments - the PWR standard primary coolant environment (less than 20ppb dissolved oxygen -DO) and the PWR doped oxygen (higher than 1ppm DO) in the refreshed autoclave loop system of flow rate 2 ml/min. The water temperature and pressure were chosen at the values of 320°C, 12 MPa for the NiMnMo piping steel and 300°C, 10 MPa for the CrNiMoV pressure vessel steel.

Tensile specimens of diameter 6 mm and gauge length 30 mm were tested at strain rates $1*10^{-6}$ s^{-1} and $5*10^{-7}s^{-1}$. Pre-cracked CT specimens 12.5 mm thick were used for constant displacement rate tests from $1.4*10^{-9}$ m/s to $2*10^{-8}$ m/s. After the tests, fracture surfaces were analysed by SEM. Separately, the electrochemical corrosion behaviour of the materials were measured.

EXPERIMENTAL RESULTS

Tensile specimen tests (SSRT). The stress - strain curves gained from the tensile tests are described in Fig.1. Mechanical properties for materials tested in low oxygen environment are equal to those tested in the air. At low DO environment no SCC were seen. In high DO the average crack growth rates were evaluated, see Fig.2. The crack tip strain rates were calculated according Ford (2).

The large amount of brittle, transgranular fracture was observed on fracture surfaces. The SCC initiated mostly from a pitting, see Fig.4. Making a longitudinal section of specimen from the both steels, the three different parts of

the crack growth - initiation, growth with secondary crack occurrence and growth with steps which could be considered as arrest lines (Fig.5) - was clearly seen. In CrNiMoV we also found two fine secondary cracks having started from the fracture surface. The only difference between CrNiMoV and NiMnMo steels seems to be in secondary cracks appearance.

Pre-cracked CT specimens (RDT). The J - R curves of specimen tested in low and high oxygen environments are shown in Fig.3. In case of CrNiMoV steel the initiation value of fracture toughness was decreased by oxygen environment to value as low as 7 kN/m. Only slight change was seen in the second steel. The maximum instantaneous crack velocities near SCC initiation vs. calculated crack tip strain rates are shown in Fig.2.

In the case of CrNiMoV, the SCC crack growth started immediately after load was commenced, at very low local stress and strain values below yield point and the crack tip strain rates about $1*10^{-7}$ s^{-1}. The crack tip strain rate was calculated employing the 3D finite element analysis as a static case. The SYSTUS program was used. The crack grew by a mechanism of SCC transgranular cleavage with the appearance of many secondary cracks. The crack path was typically very rough. The SCC cleavage facets were small, if any, and arrest lines were not observed. Short transgranular secondary cracks were seen on micrographs of fracture from a central longitudinal cut of specimen (Fig.6) on the surface.

In the NiMnMo steel the SCC crack began to propagate after some ductile dimples occurred. At this moment the crack tip was blunted and the corresponding crack tip strain rate of $2*10^{-6}$ s^{-1} was calculated. The values of strains and stresses at the crack tip were on the yield level. If specimen was sidegrooved the SCC initiated first from the sidegroove. On the fracture surface there were seen several large SCC facets including secondary cracks and low steps, see Fig.7. Also some ductile dimples appeared in the facets. Optical microscopy of the specimen section did not prove any fine cleavage secondary cracks, only one long secondary crack branched from the main crack was seen on the fracture surface. This crack started after the crack tip blunting took place. Several other short but wide secondary cracks or dimples were observed in this area as well.

DISCUSSION

SEM observation seems to confirm the idea that slip dissolution mechanism, (2), controls SCC in NiMnMo steel. As an evidence low round steps on slightly rough fracture surfaces were found out (Fig.5). Contrary, fine secondary cracks of approximately 15 μm of depth appeared on fracture surface of CTs from CrNiMoV steel. The observed transgranular, cleavage cracks cannot be explained by slip dissolution model. The cracks could be viewed as evidence of local brittle fracture events resulted from enhanced dislocation activity on inclined planes.

They seem to be reminders of the enhanced plasticity SCC mechanism operation, Magnin (3).

The observations of two different SCC mechanisms can be confirmed by Fig.3, where two lines for low and high sulphur content of the Ford's model are drawn. The average crack velocity - crack tip strain rate points of all tensile specimens can fit well the high sulphur line. Simultaneously, the line fits well all points of maximum instantaneous SCC rates from CTs of NiMnMo steel. The points of CTs of CrNiMoV steel lie above the high sulphur line and they could be influenced by another fracture mechanism.

CONCLUSIONS

Comparing SCC mechanisms of two steels in water doped oxygen, one can conclude:

- the usage of SSRT only did not fully identify the crack growth mechanism;
- slip dissolution mechanism controls SCC failure in NiMnMo steel;
- fine, cleavage secondary cracks, inclined from fracture surface by 45° were observed in CrNiMoV steel, especially in CT specimens; this confirms that an enhanced cleavage process passed through in SCC crack tip vicinity and that the enhanced plasticity mechanism was involved.

REFERENCES

(1) Dietzel W., Schwalbe K.-H.: Standardisation of Fracture Mechanics based SCC testing. Proceedings of ECF10, Berlin, 1994, pp.53 - 66.

(2) Ford P., Andresen P.L.: „Life prediction for low alloy steels subject to stress corrosion and corrosion fatigue", VGB Conference „Corrosion and Corrosion Protection in Power Plant Technology 1995", Essen, November 1995.

(3) Magnin T., Chieragatti R., Oltra R., Acta metall. mater. Vol.38, No.7, 1990, pp.1313 - 1319.

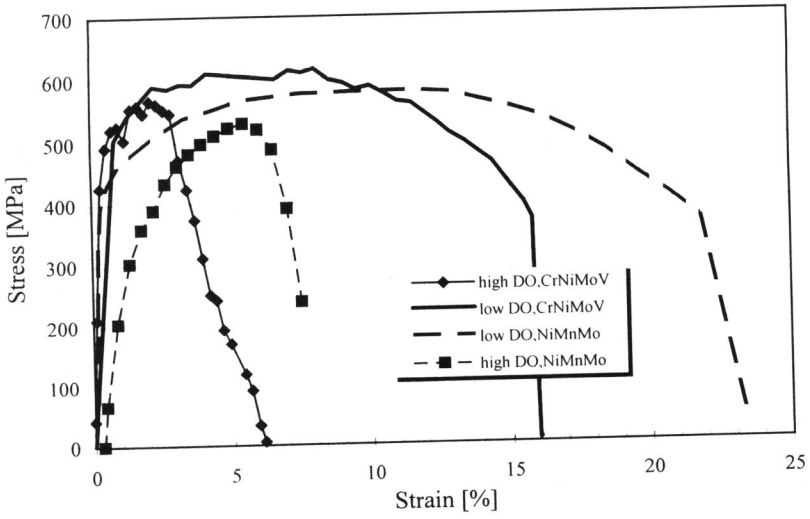

Figure 1. Results of slow strain rate tests in water environment.

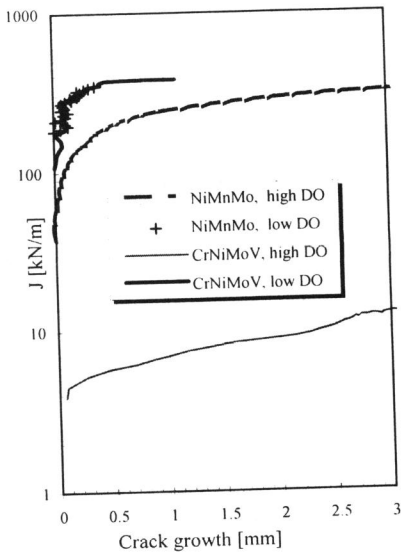

Figure 2. J-R curves in water environment.

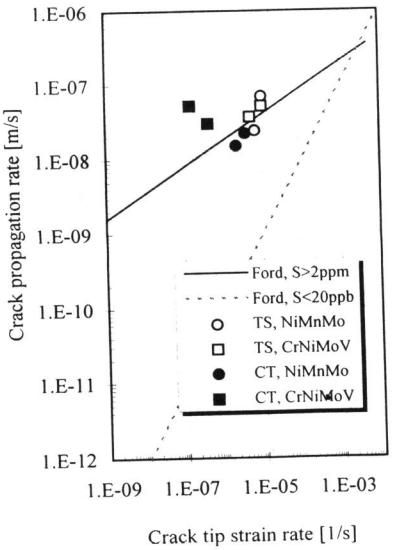

Figure 3. Theoretical and experimental data of high oxygen water.

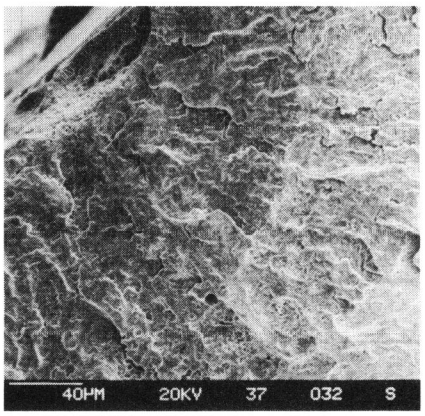

Figure 4. Crack initiation from pitting (CrNiMoV).

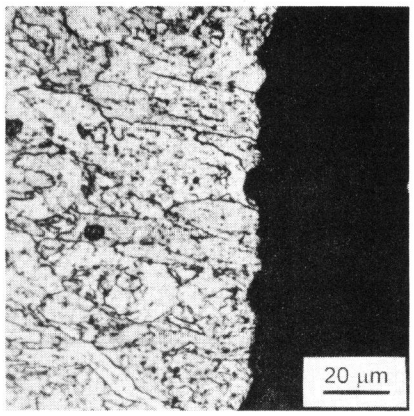

Figure 5. Section of arrest lines (NiMnMo).

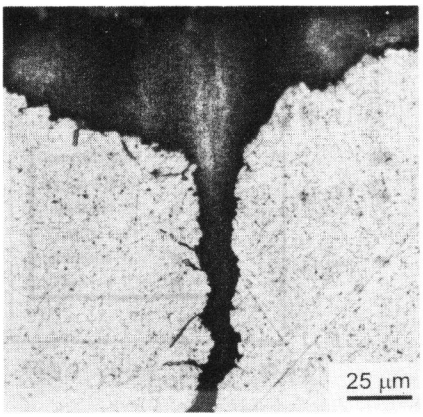

Figure 6. CrNiMoV-SCC (left) initiation from fatigue (right).

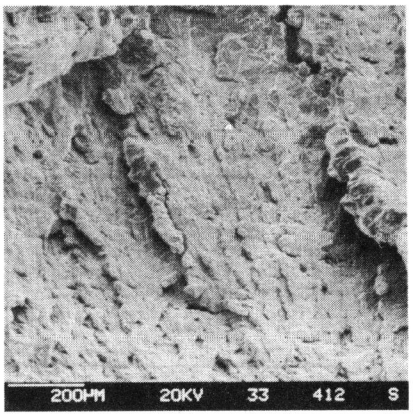

Figure 7. SCC crack propagation (NiMnMo).